CORA Cork Open Research Archive
Cartlann Taighde Oscailte Chorcaí

Title	Feasibility analysis of geothermal energy utilization in ultra-low temperature district heating networks: Effect of heat distribution in underground tunnels
Authors	Ofili, Sylvester;Alimohammadi, Hossein;Krupenski, Igor;Sameti, Mohammad;Li, Zili;Sukumaran, Sreenath;Lepiksaar, Kertu;Ledvanov, Aleksandr;Volkova, Anna
Publication date	2026-08-15
Original Citation	Ofili, S, Alimohammadi, H, Krupenski, I, Sameti, M, Li, Z, Sukumaran, S, Lepiksaar, K, Ledvanov, A & Volkova, A 2026, 'Feasibility analysis of geothermal energy utilization in ultra-low temperature district heating networks: Effect of heat distribution in underground tunnels', Renewable Energy, vol. 270, 125920, pp. 1-11. https://doi.org/10.1016/j.renene.2026.125920
Type of publication	Article (peer-reviewed)
Link to publisher's version	https://www.scopus.com/pages/publications/105038901610 - 10.1016/j.renene.2026.125920
Rights	© 2026, authors. Published by Elsevier Ltd. This is an open access article under the CC BY license (http://creativecommons.org/licenses/by/4.0/) - https://creativecommons.org/licenses/by/4.0/
Download date	2026-11-04 15:38:25
Item downloaded from	https://hdl.handle.net/10468/19528



UCC
University College Cork, Ireland
Coláiste na hOllscoile Corcaigh

Renewable Energy 270 (2026) 125920

Contents lists available at ScienceDirect

Renewable Energy

journal homepage: www.elsevier.com/locate/renene

Feasibility analysis of geothermal energy utilization in ultra-low temperature district heating networks: Effect of heat distribution in underground tunnels

Sylvester Ofili [a,*], Hossein Alimohammadi [a], Igor Krupenski [a,c], Mohammad Sameti [b], Zili Li [b], Sreenath Sukumaran [a], Kertu Lepiksaar [a], Aleksandr Ledvanov [c], Anna Volkova [a,**]

[a] Tallinn University of Technology, Department of Energy Technology, Ehitajate tee 5, Tallinn, 12616, Estonia
[b] School of Engineering and Architecture, University College Cork, Cork, Ireland
[c] EnergyMentor OÜ, Katusepapi 6, Tallinn, 11412, Estonia

ARTICLE INFO

Keywords:
Ultra-low-temperature district heating
Ground-source heat pump
Geothermal energy
Tunnels

ABSTRACT

The integration of ground-source heat pumps into ultra-low-temperature district heating networks represents a promising pathway for decarbonizing urban heat supply and mitigating the shortcomings of conventional high-temperature district heating systems. However, the feasibility of such systems depends on several technical factors related to operating conditions, demand characteristics and heat distribution. This study evaluates the technical feasibility and annual performance of a geothermal heat pump–based ultra-low temperature district heating system operating at supply and return temperatures of 35/20 °C under realistic boundary conditions. The investigated system consists of a ground-source heat pump connected to a borehole field comprising 135 boreholes, each 200 m deep, serving a district heating network with a peak demand of 5.2 MW. A system-level modelling framework implemented in MATLAB/Simulink is used, with district-heating boundary conditions derived from Leanheat® network simulations, to assess a partial peak-load coverage strategy, geothermal borefield behaviour, and the influence of network temperature level and distribution environment, including tunnel based pipe routing, on system performance. The results show that a heat pump sized to cover a fraction of the peak demand can supply approximately 69% of the annual heat demand while achieving a seasonal performance factor of 3.82. Borefield operation remains thermally feasible throughout the annual cycle, with no freezing observed at the borehole outlet. A comparative analysis shows that increasing the network temperature level to 60/40 °C results in similar demand coverage but significantly higher electricity consumption due to reduced heat pump efficiency. Furthermore, routing district heating pipes through an underground tunnel environment reduces annual distribution heat losses by approximately 183 MWh without significantly affecting heat pump performance or hydraulic behaviour. A sensitivity check shows that the tunnel environment partially offsets the increase in distribution heat losses associated with reduced pipe insulation.

1. Introduction

Heating and cooling are among the most energy- and carbon-intensive sectors in Europe and many other regions [1], accounting for approximately 40% of the EU's total gross final energy consumption [2]. As countries pursue ambitious climate goals and carbon neutrality targets, decarbonizing heat supply has become a central challenge, driving changes in how heating and cooling are produced and distributed [3]. In response, energy storage technologies [4], and renewable energy sources are increasingly considered to enhance system flexibility and reduce emissions [5].

Within this transition, district heating (DH) systems play an

This article is part of a special issue entitled: SESAAU2025 published in Renewable Energy.

* Corresponding author.
** Corresponding author.
E-mail addresses: sylvester.ofili@taltech.ee (S. Ofili), anna.volkova@taltech.ee (A. Volkova).

https://doi.org/10.1016/j.renene.2026.125920
Received 15 January 2026; Received in revised form 1 April 2026; Accepted 7 May 2026
Available online 8 May 2026
0960-1481/© 2026 The Authors. Published by Elsevier Ltd. This is an open access article under the CC BY license (http://creativecommons.org/licenses/by/4.0/).

important role in supplying heat to buildings, particularly in urban environments [6]. In the Baltic states (Estonia, Latvia and Lithuania), for example, approximately 64% of residential heat is supplied by district heating [7]. However, conventional DH systems typically rely on fossil fuel-based heat sources and operate at high supply temperatures often exceeding 90 °C, which results in high thermal losses, limited compatibility with modern low-energy buildings that require lower heating loads [8], difficulty in utilizing renewable and low-exergy heat sources, and a dependence on centralized infrastructure that limits its flexibility [3]. In this context, ultra-low temperature district heating (ULTDH), generally characterized by supply temperatures below 50 °C, has emerged as a solution to address these inefficiencies and support the transition to more sustainable, flexible, and low-carbon heating systems [9].

Shallow geothermal energy is widely used as a low exergy heat source for ULTDH systems because it is a ubiquitous, relatively stable, and environmentally friendly heat source that can be harnessed from the ground, underground structures such as tunnels [10], and other subsurface environments using ground source heat pump (GSHP) systems, and can be applied in a wide range of settings, including residential districts, mixed-use developments, and retrofit projects [11]. Despite the growing interest in shallow geothermal-ULTDH, its integration presents several technical challenges, particularly related to heat distribution within the network. Distributing geothermal heat at ultra-low temperatures requires higher mass flow rates to meet heating demand, resulting in increased pressure losses and pumping requirements compared with conventional district heating systems [12]. In addition, flow rate variations within the network can affect heat pump operation. Depending on the network operating temperature and end-use requirements, additional temperature upgrading may also be required, which can increase electricity consumption and affect overall system performance [13]. Because of these complexities, several studies have focused on advanced optimization of system design, operation, and control strategies. For example, Quirosa et al. [14] presented an approach to integrating coaxial borehole heat exchangers into ultra-low temperature district heating and cooling networks, demonstrating through a case study in southern Spain that the proposed system significantly reduces emissions and operating costs while offering improved performance. Yand and Svensen [9] conducted an energy, exergy, and economic performance optimization of an ultra-low temperature district heating system in low heat density area, combining a central heat pump with local boosters and comparing its performance to low- and medium-temperature district heating configurations. To address the economic inefficiency associated with the use of building-level booster heat pumps for domestic hot water preparation, Topal and Arabkoohsar [15] proposed an ULTDH configuration with neighbourhood-scale water-source booster heat pumps and a triple-pipe distribution network, demonstrating improved techno-economic performance through a case study. Yang et al. [16] demonstrated the influence of substation design and supplementary heating strategies on energy use in ULTDH systems by comparing the relative heat and electricity demand for domestic hot water preparation across different substation configurations.

The integration of energy geostructures with ULTDH systems can play an important role in enhancing the operational performance. Tunnels are increasingly studied in the context of district heating, for example, the Turin tunnel [17], the London Underground (LU) transport network [18] and the ground around it [19], Grand Paris Express [20], Shenzhen subway tunnels [21] and Brenner Base Tunnel [22]. Chicherin et al. [23] estimated that underground car/railway tunnels in Belgium have heat recovery potential of up to 2.9 GWh annually. Dai et al. [24] described that thermal output of energy tunnels can vary from 5 to 6 W/m^2 according to the ground temperature and fluid inlet temperature. Based on a detailed report describing design and development of heating and cooling system for a zoo building, utilizing a road tunnel (ca. 1 km length), Csesznák et al. [25] showed that heat extraction from existing tunnels can be carried out with minimal impact on environment. According to ARUP Technical Report, the ground heat exchange rate from a 600 m energy tunnel is similar to that of 35 numbers of 100 m long borehole fields [26]. Barla & Insana carried out feasibility study for the future Line of Turin Metro and reported a thermal yield between 400 and 1200 W/m under Italian geographic conditions [27]. Since the air temperature inside tunnel is higher than surrounding soil temperatures [28], tunnels also offer a potential pathway for DH pipe routing. This arrangement can reduce heat losses from distribution pipes and potentially improve the efficiency of shallow geothermal ULTDH networks. Most of the existing research focuses on energy tunnels, where tunnel linings are equipped with heat exchangers and used directly as geothermal energy sources or sinks [29]. The role of tunnels as distribution pathways for geothermal heat has received very limited attention. One existing study examines district heating pipes routed through a tunnel, but its scope is limited to structural and durability considerations of the tunnel lining, without addressing the energy-related aspects of heat distribution [30]. As a result, the energy-related implications of distributing shallow geothermal heat through tunnel in ULTDH remain insufficiently explored.

In this context, the present study focuses on an energetic and operational feasibility assessment of utilizing shallow geothermal energy in ULTDH networks using realistic district heating demand and temperature data. A scenario-based modelling and simulation framework is employed to evaluate geothermal heat distribution under different operating conditions and network temperature regimes. In addition, the study examines the performance of utilizing tunnel as distribution network, in comparison with conventional ground-buried pipe networks.

The remainder of the paper is organized as follows. Section 2 describes the integrated system configuration, modeling framework, and design methodology. Section 3 introduces the case study and the district heating network boundary conditions. The governing equations and key performance indicators are defined in Section 4. Simulation results and their interpretation are presented in Section 5. Finally, Section 6 summarizes the main findings and outlines implications for the integration of geothermal heat pumps into ultra-low-temperature district heating systems.

2. System description and design methodology

The proposed methodological framework adopted in this study is illustrated in Fig. 1. The methodology is based on design and sizing of GSHP and geothermal borefield for a real-world case study. The performance of the proposed system is analyzed by considering four different system configurations, including a tunnel-based distribution network.

2.1. GSHP-ULTDH system configuration

The investigated system consists of a GSHP coupled to ULTDH network with a peak demand of 5.2 MW and an annual heat demand of approximately 15 GWh. Heat is supplied by a shallow geothermal borefield comprising 135 boreholes, each 200 m deep. The system comprises four main subsystems: the district heating network, the heat pump unit, the geothermal borefield, and an auxiliary ground thermal rebalancing mechanism. The heat pump extracts thermal energy from the geothermal borefield and delivers heat to the district heating network. District heating demand and operating conditions are imposed as exogenous boundary conditions derived from DH network model simulations. The geothermal loop connects the borefield and the heat pump evaporator, while the condenser side supplies heat to the district heating system at the prescribed ULTDH temperature level. The geothermal loop mass flow rate is controlled to maintain a prescribed temperature difference across the borefield. A proportional–integral controller adjusts the mass flow rate based on deviations from a reference temperature difference $\Delta T_{geo,ref}$, subject to predefined minimum

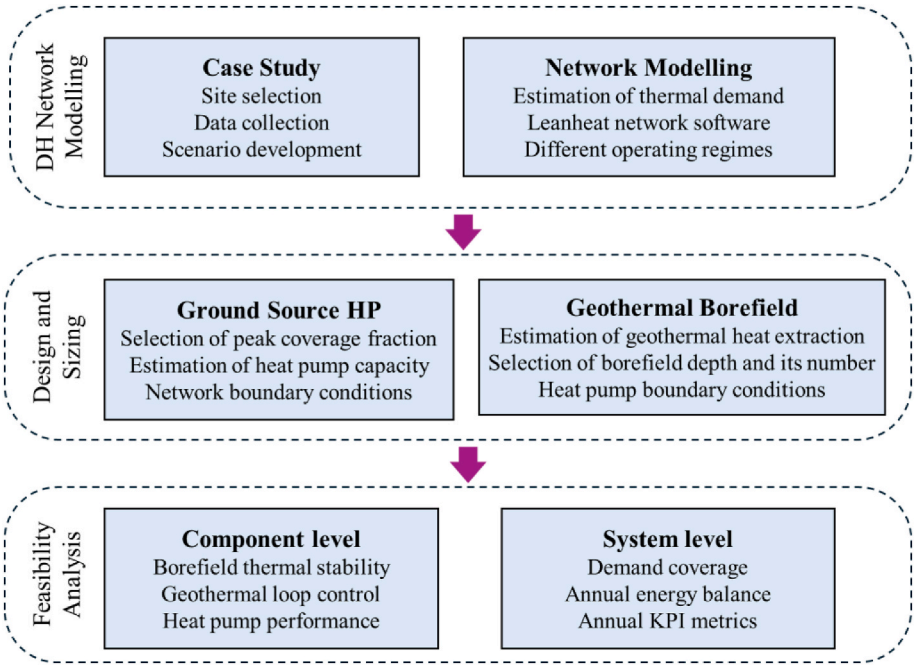


Fig. 1. Methodological framework for GSHP–ULTDH system design, modelling, and performance assessment.

and maximum flow limits. Auxiliary heat sources and detailed network hydraulics are outside the modeling scope.

2.2. Heat pump sizing and operation

The heat pump is intentionally sized to cover only a fraction of the peak district heating demand. This reflects a practical design approach in which renewable heat sources are optimized for base and intermediate loads, while auxiliary systems are used to meet short-duration peak demands. The nominal heat pump capacity $Q_{HP,max}$ is defined as in Equation (1)

$$Q_{HP,max} = f_{HP} \times Q_{DH,peak} \tag{1}$$

where $Q_{DH,peak}$ denotes the peak district heating demand extracted from Leanheat® data [31] and f_{HP} is the selected peak coverage fraction. The heat pump performance is modeled using a temperature-dependent Carnot-based formulation, allowing the coefficient of performance to vary with source and sink temperatures during the simulation. The heat pump operates in a load-following mode subject to its nominal capacity constraint. When the district heating demand exceeds $Q_{HP,max}$, the heat pump output is capped. The remaining demand is assumed to be met by auxiliary heat sources, which is outside the scope of the present study. The auxiliary heat sources are assumed to provide the required peak-load capacity under realistic operating conditions.

2.3. Thermal boundary conditions

Ground temperatures for buried district heating pipes were taken from Estonian Weather Service data and represented using monthly average values ranging from 3 to 15 °C. These temperatures correspond to typical district heating pipe installation depths of approximately 1–2 m below ground level. Air temperatures for tunnel-based pipe routing were obtained from measurements in an underground tunnel in Dublin, where hourly air temperature was recorded over a full year in 2023 and ranged between 15 and 18 °C [32]. The tunnel is located at depths of approximately 21–23 m below ground level. It consists of twin-bores, each approximately 4.5 km long and 11.7 m in diameter. Ventilation in the tunnel is provided by multiple jet fans, which induce longitudinal airflow. The data used corresponds to the innermost sensor located farthest from the tunnel entrance, where ventilation effects are minimal and the air temperature remains relatively stable and largely unaffected by outdoor air or local climatic conditions. These temperatures were applied as external thermal boundary conditions for the respective pipe environments, while pipe geometry and network layout were kept identical across all cases.

2.4. Geothermal borefield design

The geothermal source is modeled as a vertical borehole field consisting of 135 parallel boreholes, each with a depth of 200 m. The borefield sizing in this study is based on annual heat demand coverage, seasonal load variation, and a design-specific heat extraction rate per unit borehole length. The geothermal system is designed to supply the base load of the ULTDH network, while peak demand is met by auxiliary heat sources. Seasonal variations in heat demand and ground thermal response are explicitly captured through dynamic simulations over the entire heating period. Consequently, the borefield depth and number of boreholes are determined to ensure sustainable long-term heat extraction. The adopted sizing approach is based on simplified GSHP design methods using specific heat extraction rates, as commonly applied in system feasibility assessment. The nominal geothermal heat extraction is estimated as Equation (2)

$$Q_{geo,nom} = Q_{HP,max}\left(1 - \frac{1}{COP_{nom}}\right) \tag{2}$$

where COP_{nom} is the nominal heat pump coefficient of performance. The total required borehole length is then computed using Equation (3)

$$L_{tot} = \frac{Q_{geo,nom}}{q'_{geo}} \tag{3}$$

where q'_{geo} is the target specific extraction rate. The number of boreholes is determined from the total required borehole length and the fixed borehole depth.

2.5. Borefield thermal model

The borefield thermal behavior is represented using a lumped-parameter model accounting for heat transfer between the geothermal fluid, borehole wall, and surrounding ground. The model includes an effective thermal resistance and thermal capacity to capture seasonal ground temperature dynamics. Groundwater advection was neglected and heat transfer was assumed conduction-dominated. While groundwater flow may influence borefield performance in some geological settings, the present system-level feasibility analysis focuses on first-order thermal behavior.

2.6. Scenario development

Four district heating configurations were considered in this study. The reference configuration is an ULTDH system operating at 35/20 °C with conventional ground-buried distribution pipes. Keeping it as a base case, three additional configurations were analyzed: (i) an ULTDH (35/20 °C) system with tunnel-based distribution, in which the district heating pipes are routed through an underground tunnel environment; (ii) a low-temperature district heating (LTDH) system operating at 60/40 °C with ground-buried distribution pipes; and (iii) an LTDH system operating at 60/40 °C with tunnel-buried distribution pipes. Pipe insulation class II was used in all four scenarios. A schematic representation of the tunnel-based distribution configuration (case i) is shown in Fig. 2, illustrating the integration of the geothermal borefield, central heat pump, tunnel-based distribution network, and connected buildings.

3. Case study and data collection

3.1. District heating network and operating conditions

The case study represents an urban district heating network operating under an ultra-low-temperature district heating regime. The network operates at nominal supply and return temperatures of 35 °C and 20 °C, respectively. The thermal demand exhibits pronounced seasonal and short-term variability, with peak loads reaching 5.2 MW during winter and substantially lower demand during summer operation.

3.2. Network model boundary conditions

The district heating network was modeled using the Leanheat® Network Software environment [31]. High-resolution boundary conditions were derived from network simulations, providing time series of thermal demand, supply temperature, and mass flow rate at the network level. These time series are used as exogenous inputs for the GSHP–DH system model. The network simulations were performed using a quasi-steady-state hydraulic and thermal modeling approach. For each operating regime, mass flow rates were calculated to meet the imposed thermal demand while maintaining predefined supply and return temperature levels corresponding to ULTDH (35/20 °C) and LTDH (60/40 °C) operation. The district heating demand profile remained identical across all investigated scenarios. Hydraulic losses and circulation pump electricity consumption were calculated based on network pressure losses, assuming constant pump efficiency across all scenarios.

Distribution heat losses were calculated for each pipe segment as a function of the temperature difference between the pipe surface and the surrounding environment. Since heat losses from DH pipes depend on the thermal characteristics of its surrounding environment, two pipe installation environments were considered: ground-buried pipes and tunnel-installed pipes. For ground-buried pipes, soil temperature was used as the ambient reference, while tunnel air temperature was used for tunnel-installed pipes. Two insulation classes (Class I and Class II) were analyzed to assess the influence of pipe insulation on distribution losses. Tunnels constitute a distinct thermal environment compared to soil, exhibiting different temperature dynamics, airflow patterns, humidity levels, and heat transfer mechanisms [33].

The simulations were carried out for a full-year period with an hourly temporal resolution, capturing seasonal variations in thermal demand, ambient conditions, and network operating parameters. The resulting time series of mass flow rates, supply and return temperatures, distribution heat losses, and pumping electricity consumption were aggregated to obtain annual performance indicators for each investigated network configuration.

The following boundary condition time series are extracted and used as external inputs to the GSHP-DH system model:

- District heating thermal load $Q_{\text{load}}\ (t)$
- District heating supply temperature $T_{\text{sup}}\ (t)$
- District heating mass flow rate $\dot{m}_{\text{DH}}(t)$

All time series are provided at a fixed temporal resolution of 15 -minute and cover a full annual period. These boundary conditions are treated as exogenous inputs and are not influenced by the operation of the geothermal heat pump system, ensuring a clear separation between demand-side behavior and supply-side feasibility assessment.

Fig. 3 illustrates the district heating boundary conditions used to drive the GSHP-DH system, obtained from district heating network model time-series data.

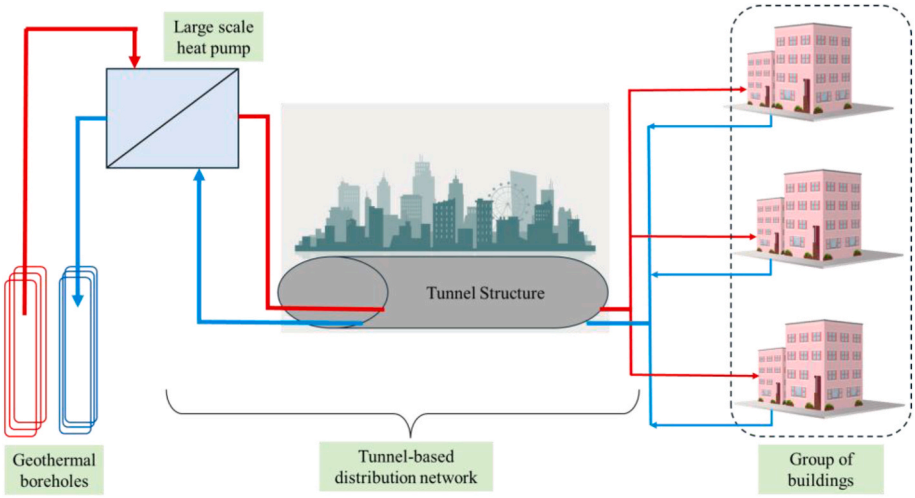


Fig. 2. Pictorial representation of geothermal based district heating system with tunnel-based distribution network (case i).

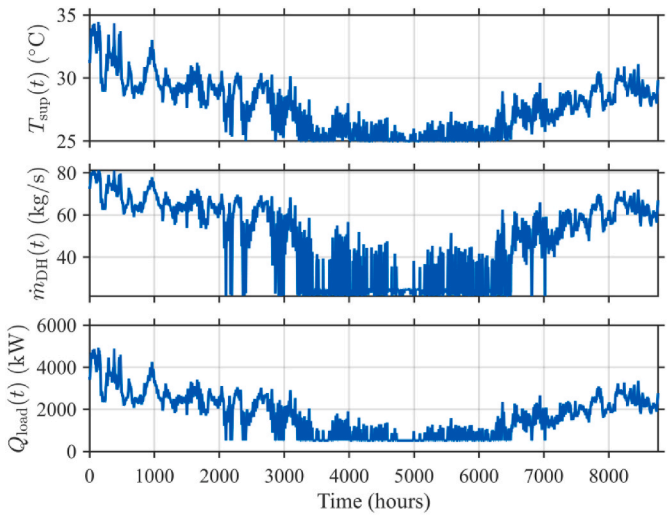


Fig. 3. District heating boundary conditions derived from DH network model including supply temperature T_{sup} (t), district heating mass flow rate $\dot{m}_{DH}(t)$, and thermal load Q_{load} (t) over the annual simulation period.

The supply temperature, mass flow rate, and thermal load exhibit pronounced seasonal and short-term variability, with peak loads occurring during winter periods and substantially lower demand during summer operation. Such boundary conditions are representative of urban district heating systems in cold-climate regions and provide a realistic operating envelope for subsequent feasibility analysis of geothermal heat pump integration into ultra-low-temperature district heating networks.

3.3. Energy demand characteristics

The total annual district heating demand represented by the model dataset amounts to approximately 15 GWh. The demand profile is dominated by space heating loads during the heating season, with comparatively low demand during summer months. The combination of high peak-to-average load ratios and frequent short-term fluctuations poses a stringent test for the operational stability and flexibility of the geothermal heat pump system.

Distribution heat losses within the DH network are represented using an effective analytical loss model calibrated against network model outputs. While dynamic thermal storage effects and transition delays are neglected at this stage, the adopted representation captures the dominant contribution of network losses to the overall energy balance and is consistent with typical performance levels reported for well-insulated ULTDH systems.

3.4. Scope and role of the case study

Fig. 4 illustrates the network topology, consumer distribution, and connection points considered in network modelling. The network consists of residential buildings (blocks of flats and flats), office buildings, and commercial consumers, resulting in a total peak demand of 5.2 MW.

Fig. 5 presents the distribution of peak thermal demand by consumer type in the investigated district heating network. In this study, flats refer to individual small residential buildings, whereas blocks of flats denote multi-apartment residential buildings with heat demand aggregated at the building level. The reported values represent the aggregated peak thermal demand of all buildings within each consumer category in the case study area. Residential buildings dominate the peak thermal load, which is characteristic of typical urban district heating systems in cold-climate regions.

4. Governing equations and performance metrics

4.1. Coupled heat pump model

The ground-source heat pump is modeled as the thermodynamic coupling element between the district-heating sink loop and the geothermal source loop. On the district-heating side, the useful heat delivered by the condenser is determined from the imposed district-heating boundary conditions as

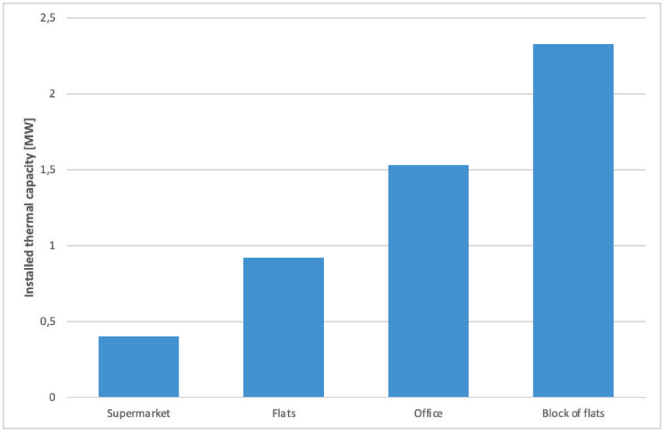


Fig. 5. Peak thermal demand by consumer type.

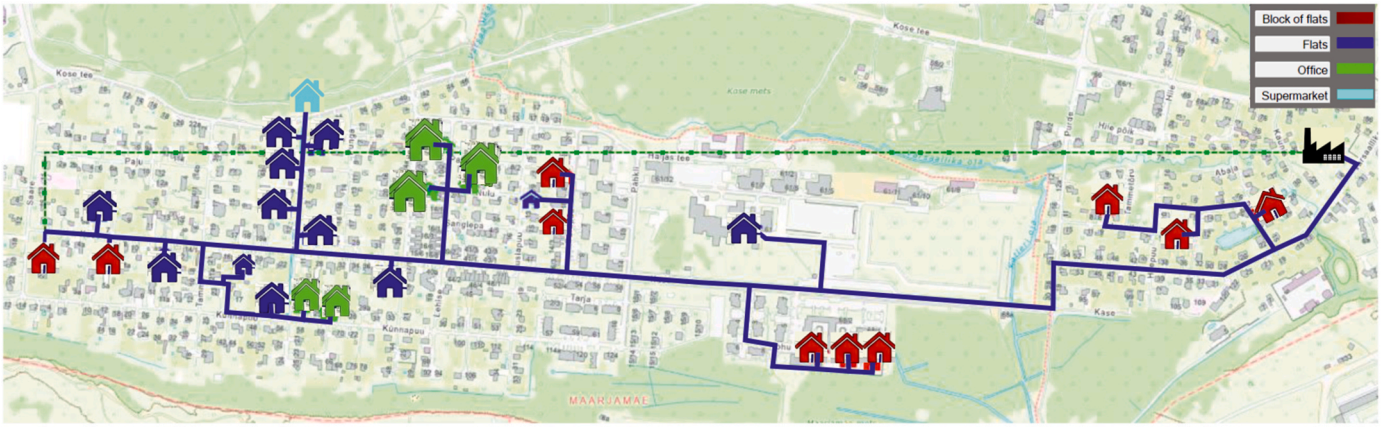


Fig. 4. Spatial layout of the investigated district heating network used as a case study.

$$Q_{HP,out}(t) = \dot{m}_{DH}(t) c_{p,w} \left[T_{sup}(t) - T_{ret}(t) \right] \quad (4)$$

where $\dot{m}_{DH}(t)$ is the district-heating mass flow rate, $T_{sup}(t)$ and $T_{ret}(t)$ are the supply and return temperatures, and $c_{p,w}$ is the specific heat capacity of water. In the present study, these district-heating quantities are obtained from Leanheat-based network simulations and treated as exogenous boundary conditions. The heat pump satisfies the instantaneous steady-state energy balance

$$Q_{HP,out}(t) = Q_{geo}(t) + P_{el}(t) \quad (5)$$

where $Q_{geo}(t)$ is the thermal power absorbed at the evaporator from the geothermal loop and $P_{el}(t)$ is the compressor electrical power. The instantaneous coefficient of performance is defined as

$$COP(t) = \frac{Q_{HP,out}(t)}{P_{el}(t)} \quad (6)$$

To capture the influence of temperature lift, the COP is expressed using a Carnot scaled formulation

$$COP(t) = \eta_{HP} \frac{T_{cond}(t)}{T_{cond}(t) - T_{evap}(t)} \quad (7)$$

where η_{HP} is an effective heat-pump efficiency factor, $T_{cond}(t)$ is the effective condenser temperature, and $T_{evap}(t)$ is the effective evaporator temperature. The condenser and evaporator temperatures are approximated from the sink-side and source-side fluid temperatures as

$$T_{cond}(t) = T_{sup}(t) + \Delta T_{app,cond} \quad (8)$$

$$T_{evap}(t) = T_{geo,out}(t) - \Delta T_{app,evap} \quad (9)$$

where $\Delta T_{app,cond}$ and $\Delta T_{app,evap}$ are lumped temperature-approach terms representing finite heat-exchanger temperature differences. Equations (7)–(9) make the interaction between the district-heating temperature level and heat-pump efficiency explicit: increasing the district-heating supply temperature raises the temperature lift and reduces the achievable COP.

4.2. Geothermal source-side model

On the evaporator side, the thermal power extracted from the geothermal loop is

$$Q_{geo}(t) = \dot{m}_{geo}(t) c_{p,geo} \left[T_{geo,in}(t) - T_{geo,out}(t) \right] \quad (10)$$

where $\dot{m}_{geo}(t)$ is the geothermal-loop mass flow rate, $c_{p,geo}$ is the specific heat capacity of the circulating brine, $T_{geo,in}(t)$ is the borefield outlet temperature entering the evaporator, and $T_{geo,out}(t)$ is the fluid temperature returning from the evaporator to the borefield.

The geothermal loop mass flow rate is regulated to maintain a prescribed temperature difference across the borefield,

$$\Delta T_{geo}(t) = T_{geo,in}(t) - T_{geo,out}(t) \quad (11)$$

subject to minimum and maximum flow-rate limits. This control strategy ensures stable source-side operation while allowing the heat extraction rate to follow the condenser-side demand imposed by the district-heating system.

4.3. Borefield thermal response and design constraints

Consistent with standard GSHP design logic, the borefield is characterized by its total active borehole length

$$L_{tot} = N_{bore} H \quad (12)$$

where N_{bore} is the number of boreholes and H is the depth of each borehole.

The nominal geothermal extraction required at design conditions is obtained from the heat-pump balance as

$$Q_{geo,nom} = Q_{HP,max} \left(1 - \frac{1}{COP_{nom}} \right) \quad (13)$$

which gives the design borehole length requirement

$$L_{tot} = \frac{Q_{geo,nom}}{q'_{geo}} \quad (14)$$

where q'_{geo} is the target specific heat extraction rate per unit borehole length.

The borefield thermal response is represented using a lumped thermal-resistance formulation in which the mean fluid temperature is related to the ground temperature and extraction load by

$$T_{geo,in}(t) = T_g(t) - Q'_{geo}(t) R_{eff} \quad (15)$$

where $T_g(t)$ is a representative ground temperature, $Q'_{geo}(t) = \frac{Q_{geo}(t)}{L_{tot}}$ is the heat extraction rate per unit borehole length, and R_{eff} is an effective thermal resistance accounting for borehole and near-ground thermal resistance.

To assess source-side feasibility, the peak specific extraction rate is evaluated as

$$q'_{geo,peak} = \frac{\max_t Q_{geo}(t)}{N_{bore} H} \quad (16)$$

and the minimum entering and leaving fluid temperatures are checked over the annual cycle. These quantities are standard indicators for determining whether the borefield remains within acceptable operating limits.

At each simulation time step, the district-heating boundary conditions $\dot{m}_{DH}(t)$, $T_{sup}(t)$, and $T_{ret}(t)$ determine the required condenser-side heat delivery through Eq. (4). The heat-pump model then computes the corresponding electrical power consumption and geothermal heat extraction using Eqs. (5)–(10). The borefield model updates the source-side fluid temperatures, which in turn affect the temperature lift and therefore the instantaneous COP. In this way, the district-heating network, heat pump, and geothermal borefield are thermodynamically coupled throughout the annual simulation.

4.4. Annual energy quantities

Annual energy quantities, obtained by time integration of the corresponding power signals as defined in Equation (17), are evaluated over the simulation period:

$$E_x = \sum_k Q_x(k) \Delta t \quad (17)$$

where $Q_x(k)$ represents the instantaneous power of interest and Δt is the simulation time step.

The following annual energy quantities are evaluated:

- Useful heat delivered by the heat pump, $E_{HP,out}$
- Heat pump electrical energy consumption, E_{el}
- Total district heating demand, $E_{DH,dem}$
- District heating distribution losses, $E_{loss,pipe}$.

4.5. Performance Indicators

To assess system-level performance and feasibility, several key performance indicators (KPIs) are defined.

The seasonal performance factor (SPF) of the GSHP is defined as in Equation (18)

$$\mathrm{SPF} = \frac{E_{\mathrm{HP,out}}}{E_{\mathrm{el}}} \tag{18}$$

The served fraction of the annual district heating demand is computed using Equation (19)

$$f_{\mathrm{served}} = \frac{E_{\mathrm{HP,out}}}{E_{\mathrm{DH,dem}}} \tag{19}$$

To assess the intensity of geothermal resource utilization, the peak specific heat extraction rate is evaluated using Equation (20)

$$q'_{\mathrm{geo,peak}} = \frac{\max_t Q_{\mathrm{geo}}(t)}{N_{\mathrm{bore}} H} \tag{20}$$

where N_{bore} is the number of boreholes and H is the depth of each borehole.

These indicators provide a compact and physically meaningful basis for evaluating the energetic efficiency, demand coverage, and thermal feasibility of GSHP integration into ultra-low-temperature district heating systems.

The integrated GSHP-DH system is implemented in a modular dynamic simulation framework and evaluated over a full annual period using a fixed 15 -minute time step. All subsystem models are executed sequentially within each time step, enabling time-resolved coupling of thermal, hydraulic, and control processes. The simulation is implemented in MATLAB/Simulink, and the resulting performance indicators fall within ranges reported for comparable ultra-low-temperature district heating systems in the literature [9]. The key model parameters and input data used in the simulations are summarized in Table 1.

5. Results and discussion

Results are first presented for the reference ULTDH configuration to demonstrate the technical feasibility of GSHP integration, followed by analyses examining how changes in distribution environment and network temperature level, affect the feasibility margin.

5.1. Borefield thermal feasibility and stability

Fig. 6 shows the temporal evolution of the geothermal borehole inlet and outlet temperatures together with a representative ground temperature. During periods of high heat extraction, the borehole inlet temperature drops below 0 °C due to brine operation, while the borehole outlet and ground temperatures remain above freezing throughout the simulation period. This indicates thermally feasible borefield operation with no freezing at the borehole wall or in the surrounding ground, as shown in Fig. 6.

Table 1
Model parameters and input data used in the GSHP–ULTDH system simulations.

Symbol	Description	Value	Unit
H_b	Borehole depth	200	m
N_b	Number of boreholes	set/computed	-
L_{tot}	Total drilled length	computed	m
R'_b	Borehole thermal resistance per unit length	0.09	$\mathrm{KmW^{-1}}$
k_g	Effective ground thermal conductivity	2.7	$\mathrm{Wm^{-1}\,K^{-1}}$
$C_{g,\mathrm{vol}}$	Ground volumetric heat capacity	2.2×10^6	$\mathrm{Jm^{-3}\,K^{-1}}$
$T_{g,0}$	Undisturbed ground temperature	10	°C
$Q_{\mathrm{HP}}^{\max}$	Rated heat-pump thermal capacity	$\alpha Q_{\mathrm{DH}}^{\max}$	W
$\mathrm{COP_{nom}}$	Nominal coefficient of performance	4.0	-
$\mathrm{COP_{min}}$, $\mathrm{COP_{max}}$	COP bounds	2.0, 6.0	-
$\Delta T_{\mathrm{geo,ref}}$	Geothermal-loop temperature-drop setpoint	3	K
$\dot{m}_{\mathrm{geo,min}}$	Minimum geothermal mass flow rate	2.0	$\mathrm{kgs^{-1}}$
$T_{\mathrm{amb}}(t)$	Ambient temperature for pipe heat-loss model (soil/tunnel)	Climate/ tunnel data	°C

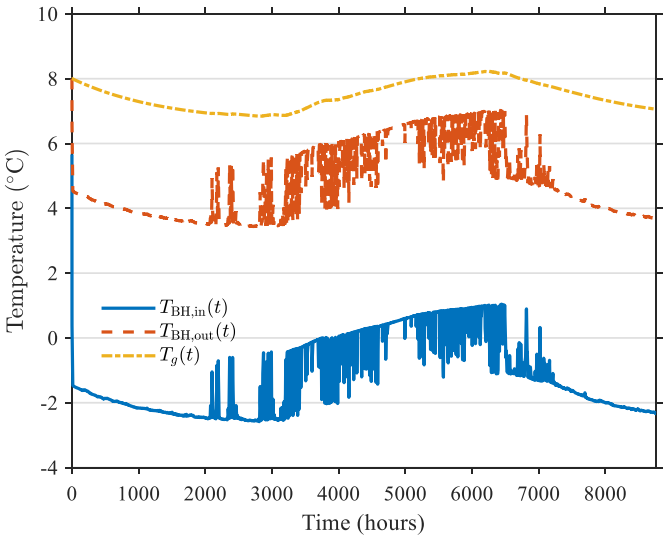


Fig. 6. Temporal evolution of geothermal borehole inlet temperature $T_{\mathrm{BH,in}}(t)$, borehole outlet temperature $T_{\mathrm{BH,out}}(t)$, and representative ground temperature $T_g(t)$ over the annual simulation period.

5.2. Geothermal loop control and operational stability

Fig. 7(a) and (b) illustrates the geothermal mass flow rate and the corresponding temperature difference across the borefield respectively. The mass flow rate is regulated within predefined bounds to maintain the target geothermal temperature difference. The temperature difference closely tracks the reference value over the annual cycle, indicating stable and well-controlled geothermal loop operation under variable district heating demand.

5.3. Heat pump performance and electrical demand

Fig. 8 presents the thermal and electrical performance of the heat pump. The delivered thermal power follows the district heating demand up to the nominal heat pump capacity, with near full-load operation

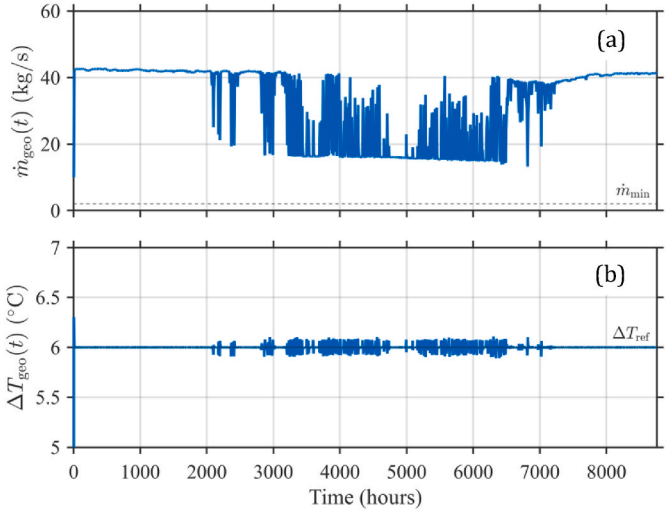


Fig. 7. Operational behavior of the geothermal loop over the annual simulation period; (a) geothermal mass flow rate $\dot{m}_{\mathrm{geo}}(t)$ regulated within prescribed bounds, and (b) geothermal temperature difference $\Delta T_{\mathrm{geo}}(t)$ tracking the reference value ΔT_{ref}.

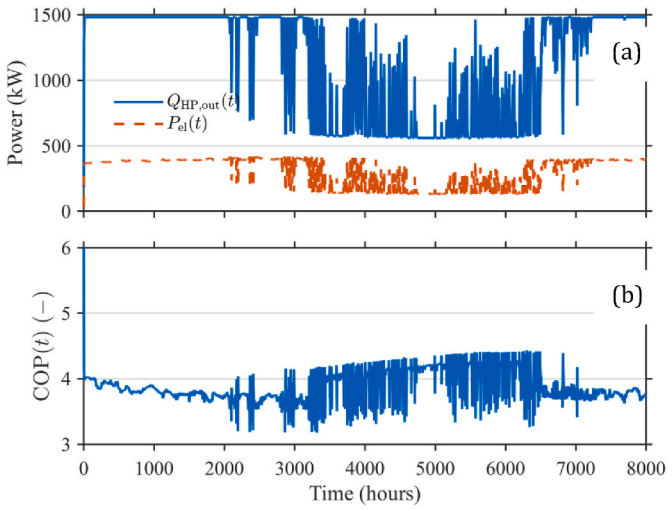


Fig. 8. Heat pump operational performance over the annual simulation period: (a) shows the delivered thermal power $Q_{HP,out}$ (t) and the corresponding electrical power consumption $P_{el}(t)$, (b) presents the time-varying coefficient of performance COP(t).

during peak demand periods as shown in Fig. 8. The coefficient of performance (COP) exhibits seasonal variation which is goverened by Eq. (7), with higher values during periods of reduced temperature lift. Overall, the heat pump operates within a realistic COP range and maintains stable performance over the annual simulation period.

5.4. Demand coverage and annual energy balance

Fig. 9 compares the district heating demand with the thermal output supplied by the geothermal heat pump. While the heat pump is sized to cover only a fraction of the peak demand, it supplies a substantial share of the annual energy demand. During peak load periods, the remaining demand is assumed to be met by auxiliary heat sources outside the scope of the present model. The ratio of the integrated areas under the two curves, representing the total annual energy demand and the energy supplied by the heat pump, is 0.69, indicating that the heat pump covers 69% of the total annual energy demand.

The resulting annual energy balance, calculated from Equation (17), and the associated KPIs (Equations (18)–(20) are summarized in Table 2 and Fig. 10. The geothermal heat pump supplies 10.37 GWh of useful

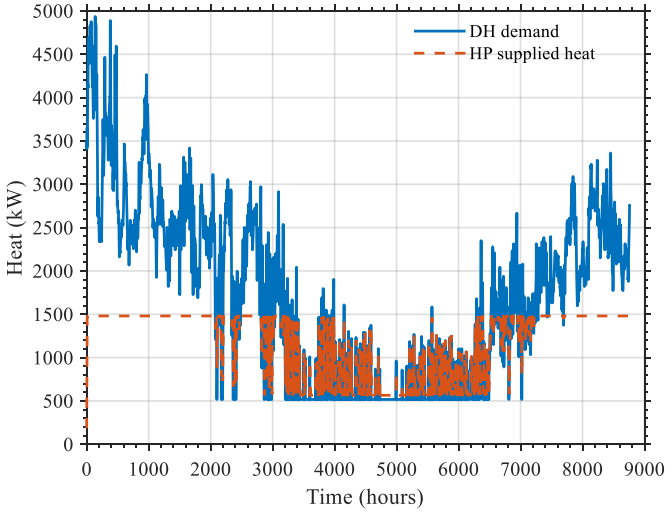


Fig. 9. Comparison between district heating demand and heat supplied by the geothermal heat pump over the annual simulation period.

Table 2
Annual key performance indicators of the GSHP-DH system obtained from a one-year simulation under district heating model boundary conditions.

Metric	Value			
	Base case: ULTDH (35/20 °C)	LTDH (60/40 °C)	LTDH (60/40 °C): DH pipe in tunnel	ULTDH (35/20 °C): DH pipe in tunnel
Useful heat delivered (HP condenser), $E_{HP,out}$	10370 MWh	10609 MWh	10576 MWh	10332 MWh
Electricity consumed (HP), E_{el}	2715 MWh	4485 MWh	4468 MWh	2701 MWh
Seasonal performance factor, SPF $= \frac{E_{HP,out}}{E_{el}}$	3.82	2.36	2.36	3.82
DH heat demand (Leanheat), $E_{DH,dem}$	14969 MWh	14969 MWh	14969 MWh	14969 MWh
DH mass flow rate	43.6 t/h	29.5 t/h	29.5 t/h	43.6 t/h
DH circ. pump elect.	319 MWh	233 MWh	233 MWh	319 MWh
Served fraction, $\frac{E_{HP,out}}{E_{DH,dem}}$	0.69	0.71	0.71	0.69
Peak HP heat output	1480.7 kW	1480.7 kW	1480.7 kW	1480.7 kW
Peak HP electric power	418.8 kW	651.5 kW	650.4 kW	417.9 kW
BH mass flow peak/p95	$\frac{42.8}{42.4\ \frac{kg}{s}}$	$\frac{33.0}{32.8\ \frac{kg}{s}}$	$\frac{33.0}{32.8\ \frac{kg}{s}}$	$\frac{42.8}{42.4\ \frac{kg}{s}}$
BH inlet temperature min/p5	$-\frac{2.6}{-2.5\,°C}$	$-\frac{1.2}{-1.1\,°C}$	$-\frac{1.2}{-1.1\,°C}$	$-\frac{2.6}{-2.5\,°C}$
BH outlet temperature min/p5	$\frac{3.4}{3.5\,°C}$	$\frac{4.8}{4.9\,°C}$	$\frac{4.8}{4.9\,°C}$	$\frac{3.4}{3.5\,°C}$
Hours with BH inlet temperature < 0°C	6756 h	5479 h	5428 h	6713 h
Hours with BH outlet temperature < 0°C	0 h	0 h	0 h	0 h

thermal energy, corresponding to approximately 69% of the total annual district heating demand of 14.97 GWh. The associated electricity consumption amounts to 2.71 GWh, resulting in a seasonal performance factor of 3.82. District heating distribution losses amount to 543 MWh, corresponding to approximately 3.5% of delivered heat. The annual energy associated with ground thermal rebalancing remains small relative to the extracted geothermal energy, indicating thermally sustainable borefield operation.

5.5. Performance of the LTDH system at 60/40 °C

To place the ULTDH results in context, a LTDH system operating at 60/40 °C was analyzed under identical demand, sizing, and control assumptions. Two distribution configurations were considered: ground-buried and tunnel-buried pipes.

Increasing the network temperature level substantially increases the temperature lift at the heat pump condenser, leading to a marked

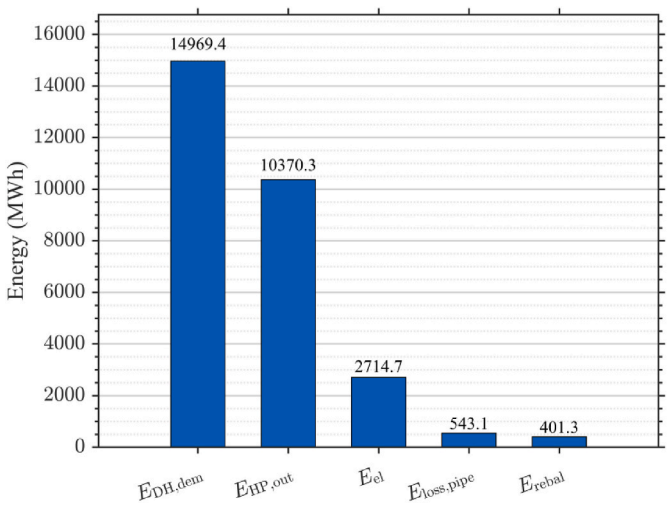


Fig. 10. Annual energy balance of the integrated GSHP-DH system.

reduction in heat pump efficiency as described by Eq. (7). Under LTDH operation, the seasonal performance factor decreases from 3.82 to 2.36, while annual electricity consumption increases from approximately 2.7 GWh to 4.5 GWh for comparable useful heat delivery (Table 2). Although the higher supply–return temperature difference reduces the required mass flow rate, this hydraulic advantage does not compensate for the efficiency penalty associated with higher operating temperatures.

Routing LTDH distribution pipes through a tunnel reduces annual distribution heat losses from approximately 1120 MWh to 950 MWh, corresponding to a decrease from 7.0% to 6.0% of delivered heat (Figs. 11 and 12). However, this reduction remains moderate and does not materially improve the overall energetic performance of the LTDH system.

While the LTDH configuration supplies a slightly higher fraction of the annual district heating demand (0.71 compared to 0.69 for ULTDH), this is achieved at the expense of substantially higher electricity consumption and increased peak electrical power demand. Overall, the results confirm that ULTDH provides a more favorable operating regime for geothermal heat pump integration when the primary objective is to maximize renewable heat utilization and minimize electricity consumption.

5.6. Effect of tunnel-based distribution on system performance

The impact of routing ULTDH distribution pipes through an underground tunnel environment is evaluated relative to the base-case configuration with ground-buried pipes. The tunnel represents a distinct thermal environment compared to soil, characterised by higher and more stable ambient temperatures [28], which can influence heat losses along the distribution network. By isolating the distribution environment while keeping all other system parameters unchanged, the following results quantify how tunnel routing affects system-level performance and the energetic feasibility of geothermal heat pump integration.

5.6.1. Distribution losses

Routing the district heating pipes through a tunnel environment reduces annual distribution heat losses from 543 MWh in the base case to 358 MWh, corresponding to a reduction from 3.5% to 2.3% of delivered heat (Figs. 11 and 12). The observed reduction in heat losses is primarily attributed to the smaller mean temperature difference between the pipe surface and the surrounding tunnel air compared to the pipe-to-soil temperature difference for ground-buried pipes. The loss difference is most pronounced during winter periods, when soil temperatures reach their lowest values while tunnel air temperatures remain comparatively stable.

As a sensitivity check, the ULTDH tunnel configuration was also evaluated using a reduced pipe insulation level (insulation class I). In this case, annual distribution heat losses increase to 433 MWh, corresponding to 2.8% of delivered heat. Despite this increase, losses remain lower than those of the ground-buried ULTDH configuration (3.5%), indicating that the tunnel environment partially offsets the effect of reduced pipe insulation (Figs. 11 and 12).

5.6.2. Heat pump performance

The reduction in distribution losses increases the fraction of geothermal heat that is effectively delivered to the buildings and slightly reduces the system-level heat production required to meet the same district heating demand. However, the impact on heat pump performance remains marginal. The COP shows no systematic change between the tunnel-based and base-case configurations, resulting in an essentially unchanged seasonal performance factor of approximately 3.82 in

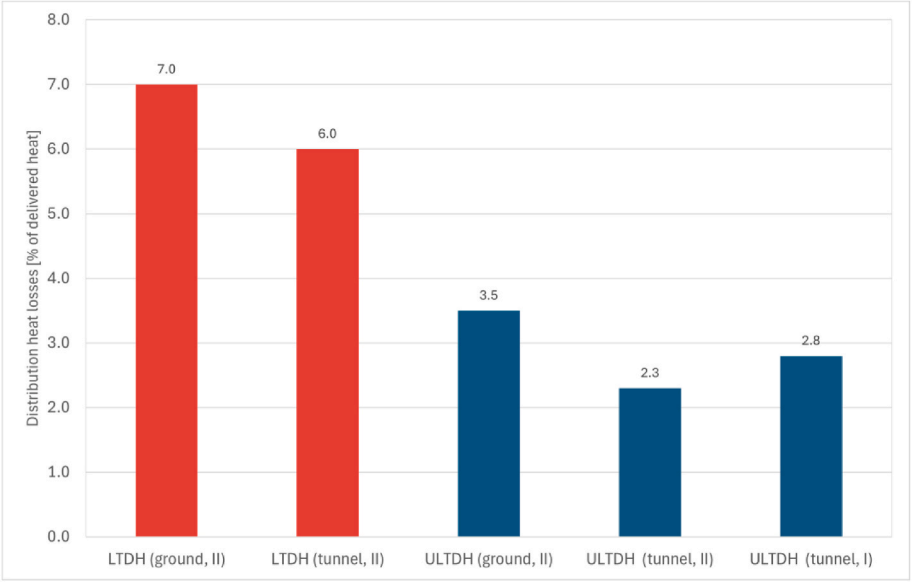


Fig. 11. Relative district heating pipe heat losses expressed as a percentage of delivered heat for all investigated scenarios.

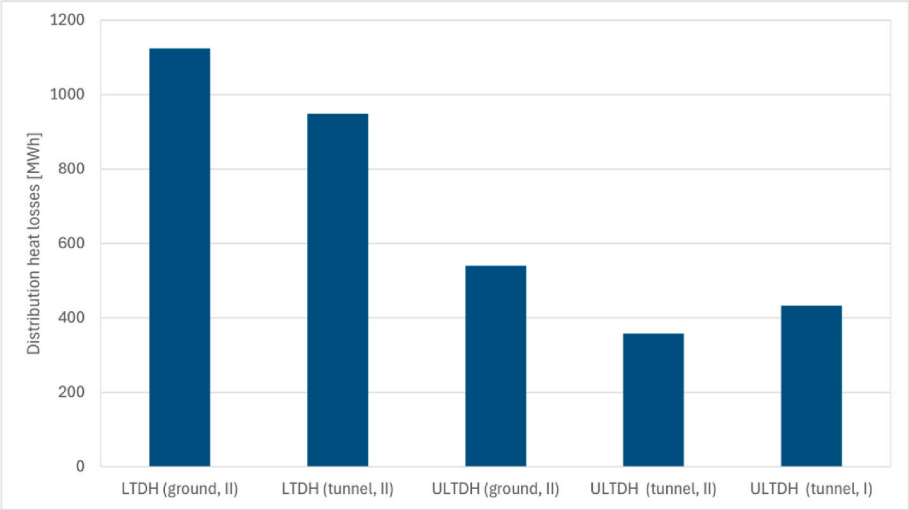


Fig. 12. Annual district heating distribution heat losses by scenario.

both cases (see Table 2). The tunnel configuration nevertheless leads to a small reduction in annual heat pump electricity consumption (from 2715 MWh/yr to 2702 MWh/yr), which is attributable to reduced distribution losses.

5.6.3. Mass flow and hydraulic implications

Table 2 shows the relationship between district heating mass flow rate and the annual electricity consumption of network circulation pumps for the analyzed configurations. As expected for ULTDH, lower network temperature operation requires relatively high mass flow rates, which in turn increase circulation pump electricity consumption. However, the increase in pumping energy remains modest compared to the overall system electricity consumption and does not offset the efficiency benefits of ULTDH. The mass flow rate and circulation pump electricity consumption are identical for the ground-buried and tunnel-buried ULTDH configurations, indicating that routing distribution pipes through a tunnel does not affect hydraulic requirements or pumping energy demand.

5.6.4. Annual energy balance and served fraction

The tunnel-based ULTDH configuration results in an annual useful heat delivery of 10333 MWh, compared to 10370 MWh in the base-case configuration, while the served fraction of the district heating demand remains unchanged at 0.69 in both cases as shown in Table 2. Although the total useful heat delivered by the heat pump is slightly lower in the tunnel case, this reflects the reduced need to compensate for distribution losses rather than a limitation in heat pump operation. Consequently, partial peak coverage by the GSHP becomes energetically more attractive when distribution pipes are routed through tunnel environments, as a larger share of the produced geothermal heat is retained within the network and delivered to end users.

5.7. Design implications and limitations

The results demonstrate that sizing a geothermal heat pump to cover only a fraction of the peak district heating demand can yield high annual energy coverage and efficient operation. This partial peak coverage strategy enables significant reductions in borefield size and capital investment while maintaining high utilization of the heat pump. The results also show that routing distribution pipes through a tunnel improves the feasibility margin of the system by reducing distribution heat losses, without requiring changes to heat pump sizing, control strategy, or hydraulic design.

Several simplifying assumptions were adopted to maintain a system-level focus, including the use of a lumped ground thermal model, simplified tunnel boundary conditions and heat pump performance, and omission of detailed hydraulic and auxiliary electrical losses. While these assumptions limit the resolution of localized effects, they are appropriate for feasibility analysis and early-stage design assessment.

6. Conclusions

This study evaluated the feasibility of integrating a ground-source heat pump into an ultra-low-temperature district heating system. It is based on realistic boundary conditions derived from district heating network simulations. A system-level modeling framework was applied to assess annual energy performance, demand coverage, electricity consumption, distribution heat losses, and geothermal borefield thermal constraints under highly variable operating conditions.

The results show that a GSHP sized to cover only a fraction of the peak district heating demand can supply a substantial share of the annual heat demand. In the investigated case, approximately 69% (10.33 GWh) of the total annual district heating energy demand is met while maintaining a seasonal performance factor of 3.8, representative of efficient large-scale GSHP operation. This confirms partial coverage of peak DH demand as an effective and practical design strategy for geothermal integration in district heating systems.

Thermal feasibility of the geothermal borefield is confirmed by the simulated temperature evolution. Although sub-zero inlet temperatures occur during peak heat extraction, borehole outlet and ground temperatures remain above freezing throughout the annual cycle, indicating thermally sustainable operation. The low supply and return temperatures (35/20 °C) of the ULTDH network play a key role in enabling efficient heat pump performance by minimizing temperature lift.

Comparison with a low-temperature district heating system operating at 60/40 °C highlights the importance of low network temperature levels. While the higher-temperature system marginally increases demand coverage, this is achieved at the expense of significantly higher electricity consumption of 4485 MWh, and reduced heat pump efficiency (COP of 2.36), confirming ULTDH as the more favorable operating regime for maximizing renewable heat utilization.

Routing ULTDH distribution pipes through an underground tunnel environment further improves the feasibility margin by reducing distribution heat losses by approximately 183 MWh annually, without significant impact on heat pump performance, hydraulic behavior, or borefield operation. This indicates that tunnel-based distribution can enhance system robustness when such infrastructure is available.

Overall, the findings demonstrate that GSHP integration into ULTDH

networks represents a technically viable and energetically efficient pathway toward low-carbon district heating. The presented framework provides practical guidance for early-stage system design by quantifying trade-offs between heat pump capacity, borefield sizing, network temperature level, and distribution environment. Future work may extend the analysis to multi-year operation and economic assessment to further support deployment decisions.

CRediT authorship contribution statement

Sylvester Ofili: Conceptualization, Data curation, Formal analysis, Methodology, Visualization, Writing – original draft, Writing – review & editing. **Hossein Alimohammadi:** Methodology, Software, Validation, Visualization, Writing – original draft. **Igor Krupenski:** Conceptualization, Software, Validation, Visualization, Writing – original draft. **Mohammad Sameti:** Conceptualization, Data curation, Writing – original draft, Writing – review & editing. **Zili Li:** Conceptualization, Funding acquisition, Writing – original draft, Writing – review & editing. **Sreenath Sukumaran:** Conceptualization, Methodology, Writing – original draft, Writing – review & editing. **Kertu Lepiksaar:** Conceptualization, Methodology, Writing – review & editing. **Aleksandr Ledvanov:** Data curation, Software, Validation, Visualization. **Anna Volkova:** Conceptualization, Data curation, Funding acquisition, Methodology, Supervision, Writing – review & editing.

Declaration of competing interest

The authors declare that they have no known competing financial interests or personal relationships that could have appeared to influence the work reported in this paper.

Acknowledgement

This work was funded under the Clean Energy Transition Partnership program TRI4: 'LEG-DHC Large-scale climate neutral Energy Geostructures in District Heating & Cooling systems/networks' and funded by Ministry of Climate of Estonia and Geological Survey Ireland. It was also co-funded by the Estonian Research Council under grants PRG2701 and TEM-TA78

References

[1] D. Schmidt, et al., Low temperature district heating for future energy systems, Energy Proc. 116 (Jun. 2017) 26–38, https://doi.org/10.1016/j.egypro.2017.05.052.
[2] European Commission, Energy performance of buildings directive. https://energy.ec.europa.eu/topics/energy-efficiency/energy-performance-buildings/energy-performance-buildings-directive_en.
[3] H. Lund, et al., 4th Generation District Heating (4GDH), Energy 68 (Apr. 2014) 1–11, https://doi.org/10.1016/j.energy.2014.02.089.
[4] S. Sukumaran, S.E. Pugal, S. Ofili, T. Kirs, M.B. Rabani, A. Volkova, Multi-Parametric analysis of a district cooling System integrated with energy storage technologies: a case Study of a university campus in Northern Europe, Environmental and Climate Technologies 29 (1) (Jan. 2025) 512–526, https://doi.org/10.2478/rtuect-2025-0035.
[5] K. Lepiksaar, G.-M. Kajandi, S. Sukumaran, I. Krupenski, T. Kirs, A. Volkova, Optimizing solar energy integration in Tallinn's district heating and cooling systems, Smart Energy 17 (Feb. 2025) 100166, https://doi.org/10.1016/j.segy.2024.100166.
[6] O. Opadokun, Y.X. Tao, J. Lamb, A review of waste heat sources for district heating, Energy Rep. 14 (Dec. 2025) 1051–1070, https://doi.org/10.1016/j.egyr.2025.07.015.
[7] A. Zajacs, et al., Utilization of geothermal energy: new possibilities for district heating networks in the Baltic states, Renew. Energy 242 (Apr. 2025) 122375, https://doi.org/10.1016/j.renene.2025.122375.
[8] D. Prando, A. Prada, F. Ochs, A. Gasparella, M. Baratieri, Analysis of the energy and economic impact of cost-optimal buildings refurbishment on district heating systems, Sci. Technol. Built Environ. 21 (6) (Aug. 2015) 876–891, https://doi.org/10.1080/23744731.2015.1040343.
[9] X. Yang, S. Svendsen, Ultra-low temperature district heating system with central heat pump and local boosters for low-heat-density area: analyses on a real case in Denmark, Energy 159 (Sep. 2018) 243–251, https://doi.org/10.1016/j.energy.2018.06.068.
[10] A. Magdy, O. Ogunleye, H. Mroueh, A. Di Donna, R.M. Singh, A review of exploiting shallow geothermal energy through tunnels: current status and future prospects, Renew. Energy 238 (Jan. 2025) 121958, https://doi.org/10.1016/j.renene.2024.121958.
[11] L. Aresti, et al., Energy geo-structures: a review of their integration with other sources and its limitations, Renew. Energy 230 (Sep. 2024) 120835, https://doi.org/10.1016/j.renene.2024.120835.
[12] T. Sommer, et al., Hydrothermal challenges in low-temperature networks with distributed heat pumps, Energy 257 (Oct. 2022) 124527, https://doi.org/10.1016/j.energy.2022.124527.
[13] T. Ommen, J.E. Thorsen, W.B. Markussen, B. Elmegaard, Performance of ultra low temperature district heating systems with utility plant and booster heat pumps, Energy 137 (Oct. 2017) 544–555, https://doi.org/10.1016/j.energy.2017.05.165.
[14] G. Quirosa, M. Torres, J.A. Becerra, F.J. Jiménez-Espadafor, R. Chacartegui, Energy analysis of an ultra-low temperature district heating and cooling system with coaxial borehole heat exchangers, Energy 278 (Sep. 2023) 127885, https://doi.org/10.1016/j.energy.2023.127885.
[15] H.I. Topal, A. Arabkoohsar, Enhancing ultra low temperature district heating systems with neighborhood-scale heat pump and triple-pipe distribution: a techno-economic analysis, J. Build. Eng. 95 (Oct. 2024) 110316, https://doi.org/10.1016/j.jobe.2024.110316.
[16] X. Yang, H. Li, S. Svendsen, Evaluations of different domestic hot water preparing methods with ultra-low-temperature district heating, Energy 109 (Aug. 2016) 248–259, https://doi.org/10.1016/j.energy.2016.04.109.
[17] Z. Wu, Y. Rui, X. Li, Y. Zhu, P. Liu, M. Yin, Numerical evaluation of thermal efficiency in harnessing heat from metro tunnels and ground, Appl. Therm. Eng. 279 (Nov. 2025) 127961, https://doi.org/10.1016/j.applthermaleng.2025.127961.
[18] H. Lagoeiro, et al., Investigating the opportunity for cooling the London underground through waste heat recovery, Build. Serv. Eng. Res. Tecnol. 43 (3) (May 2022) 347–359, https://doi.org/10.1177/01436244221084913.
[19] A. Revesz, I. Chaer, J. Thompson, M. Mavroulidou, M. Gunn, G. Maidment, Ground source heat pumps and their interactions with underground railway tunnels in an urban environment: a review, Appl. Therm. Eng. 93 (Jan. 2016) 147–154, https://doi.org/10.1016/j.applthermaleng.2015.09.011.
[20] B. Cousin, A.F. Rotta Loria, A. Bourget, F. Rognon, L. Laloui, Energy performance and economic feasibility of energy segmental linings for subway tunnels, Tunn. Undergr. Space Technol. 91 (Sep. 2019) 102997, https://doi.org/10.1016/j.tust.2019.102997.
[21] H. Cui, Y. Li, X. Bao, W. Tang, S. Wang, X. Chen, Thermal performance and parameter study of steel fiber-reinforced concrete segment lining in energy subway tunnels, Tunn. Undergr. Space Technol. 128 (Oct. 2022) 104647, https://doi.org/10.1016/j.tust.2022.104647.
[22] F. Tinti, et al., Exploitation of geothermal energy using tunnel lining technology in a mountain environment. A feasibility study for the Brenner Base tunnel – BBT, Tunn. Undergr. Space Technol. 70 (Nov. 2017) 182–203, https://doi.org/10.1016/j.tust.2017.07.011.
[23] S. Chicherin, GIS-Driven methods for scouting sources of waste heat for fifth-generation district heating and cooling (5GDHC) systems: railway/highway tunnels, Processes 13 (1) (Jan. 2025) 165, https://doi.org/10.3390/pr13010165.
[24] X. Dai, A. Bidarmaghz, G.A. Narsilio, Energy tunnels: a review of the state of the art and knowledge gaps to harness renewable energy from underground infrastructure, Tunn. Undergr. Space Technol. 142 (Dec. 2023) 105431, https://doi.org/10.1016/j.tust.2023.105431.
[25] A. Csesznák, R. Järschke, M. Wittke, B 10 Rosenstein Tunnel – designing a geothermal energy system in a spa protection area/B 10-Rosensteintunnel – planung einer Geothermieanlage im Heilquellenschutzgebiet, Geomech. Tunnelling 9 (5) (Oct. 2016) 458–466, https://doi.org/10.1002/geot.201600033.
[26] Ove Arup & Partners Limited, ARUP technical report. https://indico.cern.ch/event/1173667/attachments/2465651/4228155/Task%201-%20Thermal%20tunnel%20report_Issue_20220518.pdf.
[27] M. Barla, A. Insana, Energy tunnels as an opportunity for sustainable development of urban areas, Tunn. Undergr. Space Technol. 132 (Feb. 2023) 104902, https://doi.org/10.1016/j.tust.2022.104902.
[28] M. Barla, A. Di Donna, A. Perino, Application of energy tunnels to an urban environment, Geothermics 61 (May 2016) 104–113, https://doi.org/10.1016/j.geothermics.2016.01.014.
[29] M. Barla, A. Di Donna, Energy tunnels: concept and design aspects, Undergr. Space 3 (4) (Dec. 2018) 268–276, https://doi.org/10.1016/j.undsp.2018.03.003.
[30] T. Kasper, C. Edvardsen, G. Wittneben, D. Neumann, Lining design for the district heating tunnel in Copenhagen with steel fibre reinforced concrete segments, Tunn. Undergr. Space Technol. 23 (5) (Sep. 2008) 574–587, https://doi.org/10.1016/j.tust.2007.11.001.
[31] Danfoss, Leanheat® network. https://www.danfoss.com/en/products/dhs/software-solutions/danfoss-leanheat-software-suite-services/leanheat-network/.
[32] Mohammad Sameti, Tao Fan, Anna Volkova, Zili Li, Large-scale climate-neutral district heating and cooling: Integration of local microgrids for thermal distribution, Energy Conversion and Management: X 30 (2026) 101552, https://doi.org/10.1016/j.ecmx.2026.101552, 101552, https://linkinghub.elsevier.com/retrieve/pii/S2590174526000358.
[33] Chao Yang, Fang-Le Peng, Kai Xu, Li-Ning Zheng, Feasibility study on the geothermal utility tunnel system, Sustainable Cities and Society 46 (2019) 101445, https://doi.org/10.1016/j.scs.2019.101445, 101445, https://linkinghub.elsevier.com/retrieve/pii/S2210670718317190.